www.ietdl.org

Published in IET Microwaves, Antennas & Propagation
Received on 4th March 2012
Revised on 24th July 2012
doi: 10.1049/iet-map.2012.0124

ISSN 1751-8725

Three-way signal divider with tunable ratio for adaptive transmitting antenna arrays

A. Abbosh L. Guo

School of ITEE, The University of Queensland, Brisbane QLD4072, Australia
E-mail: a.abbosh@uq.edu.au

Abstract: A tunable wideband three-way signal divider that is useful in adaptive transmitting arrays is presented. The design of the proposed device is based on using three stepped-impedance coupled microstrip lines that have controllable coupling factors, and thus a variable signal ratio at the three output ports. The variation in the coupling factors is achieved by using two varactor diodes that are connected between the central coupled line and each of the side lines. The biasing voltages of the varactor diodes are used to control their capacitors and thus to achieve the required output signal ratios. A signal-flow analysis is used to predict the performance of the proposed device, whereas the conformal mapping technique is used to obtain the required dimensions of the coupled structure and the varactors' capacitors. The validation of the proposed design method is tested by simulations and measurements. The results indicate the possibility of changing the signal ratio across a wide range of values with more than 10 dB return loss at the four input/output ports and isolation between the output ports across more than 85% fractional bandwidth.

1 Introduction

Adaptive arrays are widely used for many purposes, such as to achieve extremely low-sidelobes or to optimise the radiation pattern for certain required characteristics concerning, for example, the gain or signal-to-noise ratio subject to the existence of noise sources or external interferences [1–4].

Two of the important applications of transmitting arrays that need pattern optimisation are the multiple-input multiple-output (MIMO) systems and retrodirective arrays [1–3]. In MIMO systems, the pattern, for example, is synthesised to transmit data to a single user while placing nulls in the directions of other users [2, 3]. In retrodirective arrays, the transmitting patterns are adapted to optimise the transmission subject to some received signal or noise distribution [1]. They find applications in many commercial and military systems, such as electronic traffic and toll management, wireless power transmission, advanced digital mobile communication systems, where limited tracking without a priori knowledge of the source is required, and many more [2, 4].

The adaptation of the array's pattern can be realised by real-time phase and/or amplitude weighting of the signals fed to the elements of the array. In this paper, a device is proposed to enable changing the amplitude of the signals in an efficient and simple manner.

The conventional scenario to implement amplitude–weight pattern optimisation on a transmitting array is to use as many variable gain amplifiers as transmitting antenna elements (Fig. 1*a*). The gain of those amplifiers is varied as per the amplitude weights required to generate a certain pattern. Obviously, this solution requires the use of a large number of variable-gain amplifiers. The other proposed solution depicted in Fig. 1*b* is to have one fixed-gain amplifier for the whole system, whereas the signal is distributed among the antenna elements using a multiway signal divider with tunable amplitude ratio at its output ports. This configuration is useful for low-power levels. For high-transmitting-power levels, the configuration shown in Fig. 1*c* that includes an easy-to-design fixed-gain amplifier for each antenna element and a variable-ratio multiway signal divider to control the amplitude weights is more realistic.

Reviewing the literature shows that there are several methods proposed to build tunable two-way signal dividers and couplers [5–8]. Most of the available designs of tunable two-way dividers are based on the theory proposed in 1958 [5], which states that the series connection of two 3-dB directional couplers using a variable phase shifter results in a tunable power divider. Concerning multiway (three-way or more) signal dividers, several configurations have been proposed to build wideband and cost-effective devices [9–18]. However, all those devices have fixed signal division, and thus, are not suitable as an implementation tool for the pattern optimisation of adaptive arrays based on amplitude weights.

In [15, 19], novel couplers and power dividers utilising coupled structures are proposed. In those designs, a chip capacitor is connected between the coupled lines at the centre of the structure to achieve a certain value for the coupling factor without the need to use narrow gaps or lines that are difficult to manufacture. If that capacitor is replaced with a varactor diode, it could be possible to change the coupling factor of the structure, and thus the amplitude ratio of the output signals, by changing the biasing voltage applied to the diode. Thus, signal dividers

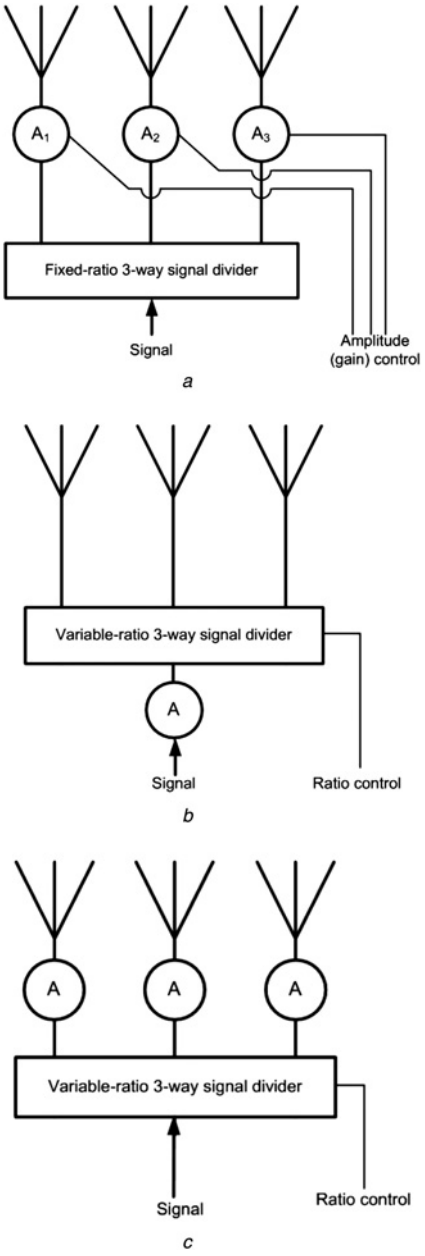

Fig. 1 *Adaptive transmitting array using amplitude weights*

a Conventional approach
Proposed approaches using three-way signal divider with tunable amplitude ratio
b For low-power levels
c For high-power levels

with tunable amplitude ratio can be realised using that approach with a properly designed coupled structure.

In this paper, a wideband three-way signal divider with planar structure and variable amplitude ratio at its three output ports is proposed. The device is based on three parallel-coupled microstrip lines. Unlike the available tunable two-way dividers that need cascading multiple couplers or dividers and variable phase shifters, the tenability of the proposed three-way divider is achieved by the direct control of the coupling factor between those three lines. That target is realised by connecting two varactor diodes between the coupled lines. A complete design method based on the signal flow diagrams and quasi-static approach is presented. The designed device has a compact size, planar structure and tunable amplitude ratio across more than 85% fractional bandwidth.

2 Theory

Assume that there are three stepped-impedance coupled lines as shown in Fig. 2. The coupled stepped-impedance structure is proven to be useful in extending the bandwidth of coupled devices [19, 20]. Those lines can be arranged in a parallel-coupled structure for uniplanar configuration [15] or broadside-coupled structure for multilayer configuration [13, 16]. Each of the three coupled lines includes three sections. The two side sections are similar with a length of l_1, whereas the central section has a length l_2 as depicted in Fig. 2. Assume that based on the dimensions of the side sections, the electromagnetic coupling factor between the three lines forming them is equal to c_s. The central section is assumed to have a coupling factor c_{12} with the upper-side line and $c_{13}$with the lower-side line.

The structure shown in Fig. 2 can be analysed using a combination of even–odd mode analysis using the quasi-static approach and signal-flow diagrams [19, 20]. In the following analysis of the three-line coupled structure, it is assumed that all the six ports of the structure are perfectly matched. Moreover, the coupling between the side lines is assumed to be negligible. The input signal at port 1 is divided between the three output ports 2, 3 and 4 and no signal appears at the ports (5 and 6), which can then be terminated by matched loads. The division of the signal between the three output ports follows the following scattering parameters, which are derived using the signal flow of multiport devices at a certain frequency with effective wavelength λ_e.

$$S_{21} = \alpha_1 + \beta_2\,\beta_6\left[\frac{\alpha_1\beta_3\beta_4}{1-\alpha_1\alpha_4-\alpha_1\alpha_6}+\alpha_5\right] \tag{1}$$

$$S_{31} = \alpha_1 + \beta_2\,\beta_6\left[\frac{\alpha_1\beta_3\beta_5}{1-\alpha_1\alpha_4-\alpha_1\alpha_6}+\alpha_3\right] \tag{2}$$

$$S_{41} = \frac{\beta_1\beta_3\,\beta_6}{1-\alpha_1\alpha_4-\alpha_1\alpha_6} \tag{3}$$

where

$$\alpha_1 = \frac{\mathrm{j}c_s\sin(2\pi l_1/\lambda_e)}{\sqrt{1-2c_s^2}\cos(2\pi l_1/\lambda_e)+\mathrm{j}\sin(2\pi l_1/\lambda_e)} \tag{4}$$

$$\alpha_2 = \frac{\mathrm{j}c_s\sin(2\pi l_1/\lambda_e)}{\sqrt{1-c_s^2}\cos(2\pi l_1/\lambda_e)+\mathrm{j}\sin(2\pi l_1/\lambda_e)} \tag{5}$$

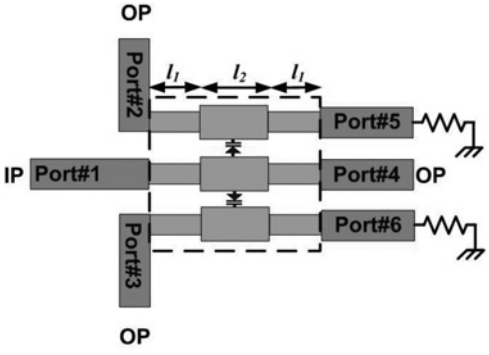

Fig. 2 *Diagram of the proposed signal divider*

$$\alpha_3 = \frac{jc_{21}\sin(2\pi l_2/\lambda_e)}{\sqrt{1-(c_{21}^2+c_{31}^2)}\cos(2\pi l_2/\lambda_e)+j\sin(2\pi l_2/\lambda_e)} \quad (6)$$

$$\alpha_4 = \frac{jc_{21}\sin(2\pi l_2/\lambda_e)}{\sqrt{1-c_{21}^2}\cos(2\pi l_2/\lambda_e)+j\sin(2\pi l_2/\lambda_e)} \quad (7)$$

$$\alpha_5 = \frac{jc_{31}\sin(2\pi l_2/\lambda_e)}{\sqrt{1-(c_{21}^2+c_{31}^2)}\cos(2\pi l_2/\lambda_e)+j\sin(2\pi l_2/\lambda_e)} \quad (8)$$

$$\alpha_6 = \frac{jc_{31}\sin(2\pi l_2/\lambda_e)}{\sqrt{1-c_{31}^2}\cos(2\pi l_2/\lambda_e)+j\sin(2\pi l_2/\lambda_e)} \quad (9)$$

$$\beta_1 = \frac{\sqrt{1-2c_s^2}}{\sqrt{1-2c_s^2}\cos(2\pi l_1/\lambda_e)+j\sin(2\pi l_1/\lambda_e)} \quad (10)$$

$$\beta_2 = \frac{\sqrt{1-c_s^2}}{\sqrt{1-c_s^2}\cos(2\pi l_1/\lambda_e)+j\sin(2\pi l_1/\lambda_e)} \quad (11)$$

$$\beta_3 = \frac{\sqrt{1-(c_{21}^2+c_{31}^2)}}{\sqrt{1-(c_{21}^2+c_{31}^2)}\cos(2\pi l_2/\lambda_e)+j\sin(2\pi l_2/\lambda_e)} \quad (12)$$

$$\beta_4 = \frac{\sqrt{1-c_{21}^2}}{\sqrt{1-c_{21}^2}\cos(2\pi l_2/\lambda_e)+j\sin(2\pi l_2/\lambda_e)} \quad (13)$$

$$\beta_5 = \frac{\sqrt{1-c_{31}^2}}{\sqrt{1-c_{31}^2}\cos(2\pi l_2/\lambda_e)+j\sin(2\pi l_2/\lambda_e)} \quad (14)$$

$$\beta_6 = \frac{\beta_1}{1-\alpha_2\alpha_3-\alpha_2\alpha_5-\alpha_1\alpha_2\beta_3(\beta_4+\beta_5)/(1-\alpha_1\alpha_4-\alpha_1\alpha_6)} \quad (15)$$

The performance of the proposed three-way signal divider is calculated using the derived model for different values of the lengths and coupling factors. It is found that the following equation derived previously in [19, 20] concerning the relation between the length of the side sections (l_1) and the length of the central section (l_2) for a wideband performance of four-port devices is still valid in the proposed six-port device for a wideband operation

$$l_2 = 2l_1 \quad (16)$$

As with the analysis in [20], the total length of the coupled structure is equal to one-third of the effective wavelength at the centre of the required operational bandwidth.

The calculated performance for different values of the coupling factors is shown in Figs. 3–5 across one-octave frequency band. It is clear from Figs. 3 and 4 that fixing the value of c_s and c_{21} (or c_{31}) while changing the value of c_{31} (or c_{21}) causes a significant variation in the level of signals emerging from the output ports 4 and 3 (or 2), whereas the level of the signal at port 2 (or 3) varies slightly. Those results can be explained by the fact that increasing the coupling factor from the central line to any side line increases the signal emerging from the output port connected to that side line, and consequently decreases the remaining signal emerging from the output port connected to the central line (port 4). To be able to change the signal level at any ratio between the three output ports, the coupling factors c_{21} and c_{31} are to be changed together as indicated in the results of Fig. 5.

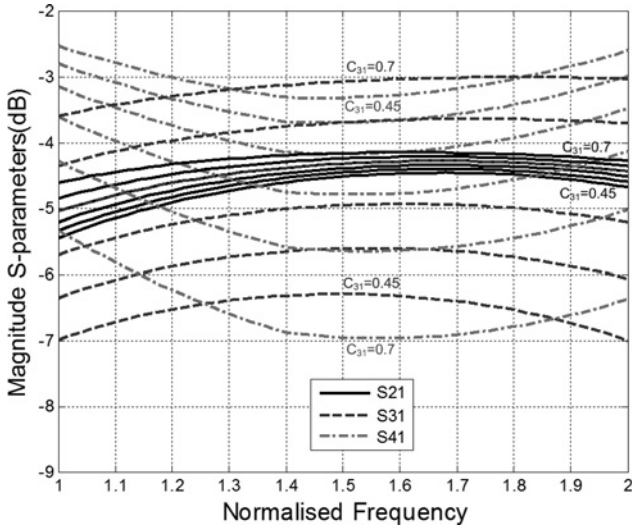

Fig. 3 *Signal level at the three output ports when $c_s = 0.45$, $c_{21} = 0.6$ and c_{31} is variable from 0.45 to 0.7*

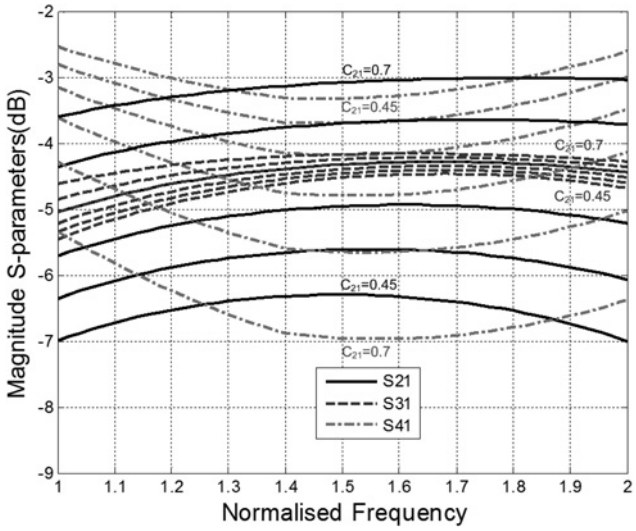

Fig. 4 *Signal level at the three output ports when $c_s = 0.45$, $c_{31} = 0.6$ and c_{21} is variable from 0.45 to 0.7*

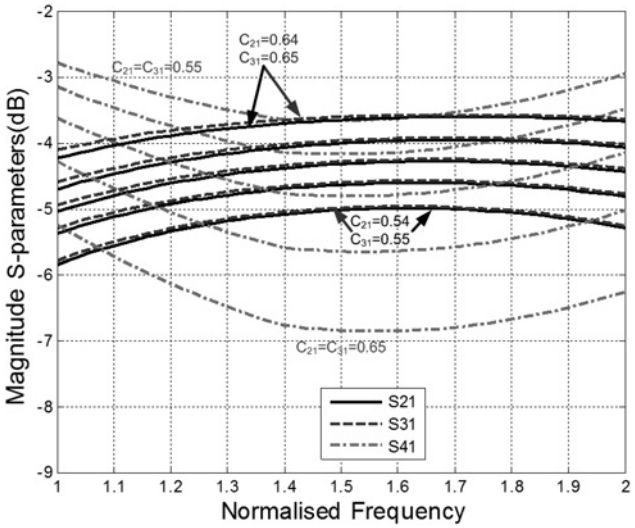

Fig. 5 *Signal level at the three output ports when $c_s = 0.45$, whereas c_{21} and c_{31} take different values from 0.54 to 0.65*

doi: 10.1049/iet-map.2012.0124

The signal ratio can also be controlled by changing the coupling factors of the first and third sections, while fixing that factor for the central section. However, there is a practical implication of that approach in that the number of varactor diodes is larger and this means an increase in the losses because of the parasitic elements of those diodes in addition to complicating the biasing circuit.

3 Design

The tunable ratio of signals can be achieved as explained earlier by changing the coupling factors of the central coupled section. The ideal scenario for that change to happen while keeping the perfect matching between the whole coupled structure and the impedance (Z_o) of the input/output ports, is to vary both of the odd–odd and even–even mode impedances of the central section (Z_{oo}, Z_{ee}) so that at any coupling factors, and thus at any signal ratio, the following equation holds [20]

$$\sqrt{Z_{ee}Z_{oo}} = Z_o = 50\ \Omega \tag{17}$$

Practically, this target can be implemented by using five varactor diodes to control the coupling factors of the central section. Two of those diodes are connected from the central line to the two side lines, whereas the three remaining diodes are connected between each of the three-coupled lines and the ground. By properly changing the biasing voltages of the five varactor diodes, the perfect matching can be maintained across the required range of signal ratios. However, this solution complicates the design as it requires five different biasing voltages to control the capacitance of the utilised varactor diodes.

The other solution is to use only two diodes connecting the central line to the two side lines. Those diodes are used to vary the odd–odd mode impedance of the central section. The even–even mode impedance is designed to have a reasonable high value that can guarantee a proper matching. To avoid using narrow gaps or lines that makes the manufacturing process difficult, the high value for the even–even mode impedance can be realised by using a slotted ground underneath the central coupled structure [20]. The dimensions of the coupled structure are calculated so that a perfect matching is achieved at three-equal signal outputs, that is, signal ratio of 1:1:1. For other ratios, the capacitor of each of the varactor diodes can take values that are above or below the required value at the 1:1:1 ratio. A compromise between the performances at the different signal ratios can be obtained using a suitable full-wave electromagnetic simulator so that an acceptable performance can be maintained at all the possible signal ratios.

The final adopted design is depicted in Fig. 6*a*. The top layer contains three parallel-coupled microstrip lines, whereas a slotted ground plane is located at the bottom layer directly underneath the central coupled section. In order to feed the diodes, a proper biasing circuit is included in the design as revealed in Fig. 6*a*.

The dimensions of the coupled structure of Fig. 6*a* can be calculated using the even–even, odd–odd and even–odd mode approach [15, 20, 21]. Assuming a quasi-transverse electromagnetic propagation, the electrical characteristics of the coupled lines (mode impedances and thus the coupling factors) can be calculated from the effective per unit length capacitances of lines and the phase velocity on the lines. In turn, the values of different mode capacitors can be

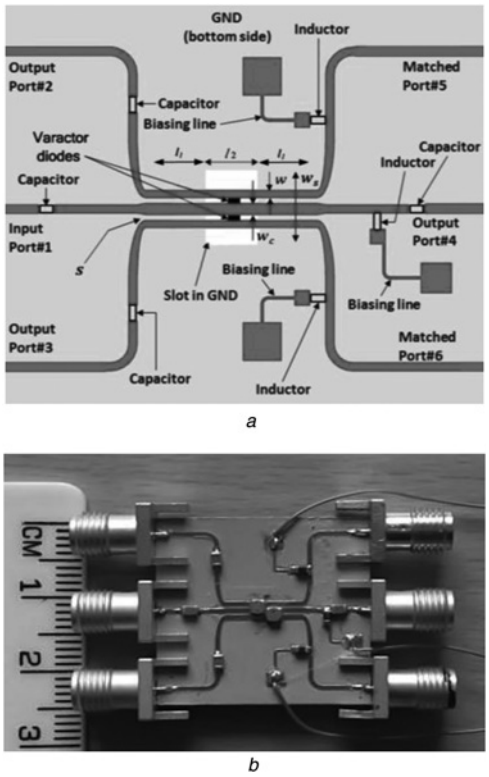

Fig. 6 *Design showing dimensions of the utilised structure and the biasing circuit and developed device*

a Outline of the final design showing dimensions of the utilised structure and the biasing circuit
b Developed device

calculated using conformal mapping techniques as explained in [21, 22]. The main parameters that define the values of those capacitors are the thickness and dielectric constant of the substrate (h and ε_r), and the dimensions of the coupled structure (s, w, w_s and w_c) depicted in Fig. 6*a*. Based on that approach, the required dimensions of the three sections and the required varactors' capacitors are found assuming a signal ratio of 1:1:1. The final dimensions are then obtained via the optimisation feature of the software HFSS. Assuming the use of the substrate Rogers RT6010 ($\varepsilon_r = 10.2$, $h = 0.635$ mm), the optimised dimensions in (mm) for a signal divider operating across the band from 2 to 5 GHz are $l_1 = 2.7$, $s = 0.21$, $l_2 = 4.8$, $w_s = 4.9$, $w = 0.89$, $w_c = 0.44$ and varactors' capacitors at 1:1:1 signal ratio $C_{v1} = C_{v2} = 1$ pF. The overall dimensions of the device are 30 mm × 30 mm.

The range across which the signal level at each of the output ports can be controlled depends on the range of the capacitor of the utilised varactor diodes. A large capacitor range means wide range of signal levels that can be achieved at each output port. To control the signal at any of the output ports by a ratio (maximum value/minimum value) of 3, the required capacitors (C_{v1} and C_{v2}) of the utilised varactor diodes should cover the range from 0.4 to 1.8 pF. Those values are evenly distributed around the required value for a signal ratio of 1:1:1 and this justifies the use of the 1:1:1 ratio as the starting design point.

4 Results and discussions

The performance of the designed device is tested via full-wave electromagnetic simulations. Also, a prototype is

developed (Fig. 5*b*) and tested. To realise the optimised range of values for the capacitors of the varactor diodes, the hyper–abrupt junction diode MA46H201 is used in the developed device. The maximum biasing voltage for this diode is 20 V.

The simulated performance of the designed three-way signal divider is shown in Figs. 7–9 for varactor capacitors that are changed from 0.4 to 1.8 pF. It is clear from the results of Fig. 7, which includes limited steps of the capacitor values for clarity of the figure, that the ratio of the signals at the three output ports can be controlled across a wide range. The deviation in the values is around ± 0.5 dB from the median value of each ratio across the band from 2 to 5 GHz. It is interesting to see that the general variations in the simulated signal levels at the three output ports (Fig. 7) agree well with the predictions using the derived theoretical model (Fig. 5) despite the fact that the derived model assumes an ideal substrate, perfect matching at all the ports and no coupling between the side lines.

The simulated reflection coefficient at all the ports of the device (owing to symmetry S44 = S11) in all the cases is below −10 dB as shown in Fig. 8. There is also a good isolation, which is more than 13 dB between the output ports 2 and 4 or ports 3 and 4 in all the investigated cases as depicted in Fig. 9. The isolation between the output ports is an important factor to prevent any signal reflected from any of the antenna elements of the array depicted in Fig. 1*b* from affecting the performance of the other antennas in the array. The isolation between the output ports 2 and 3 is more than 10 dB in most of the cases. The only case which causes the isolation to be around 9 dB is when the biasing voltages at the varactor diodes are close to zero and thus the varactors have the largest capacitor value.

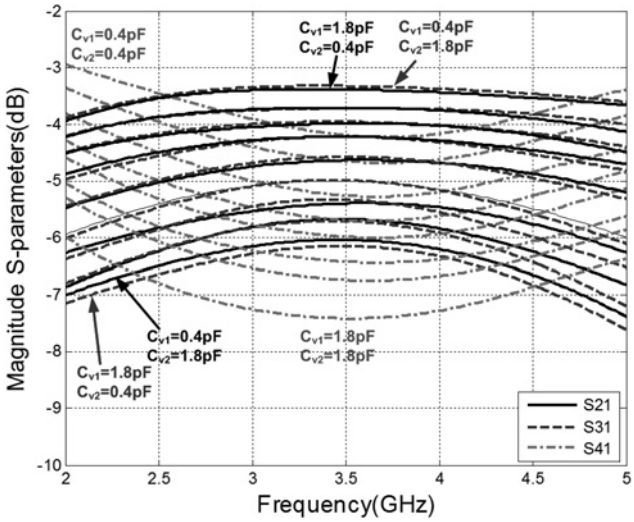

Fig. 7 *Simulated signal level at the three output ports for different values of the varactors' capacitors*

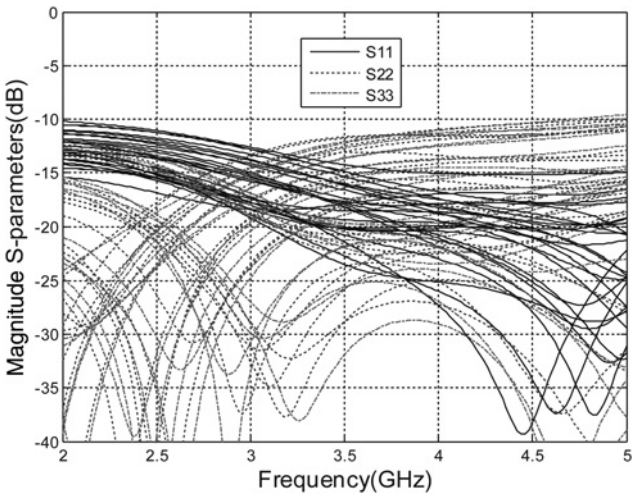

Fig. 8 *Simulated reflection coefficient at the input and output ports for different values of the varactors' capacitors*

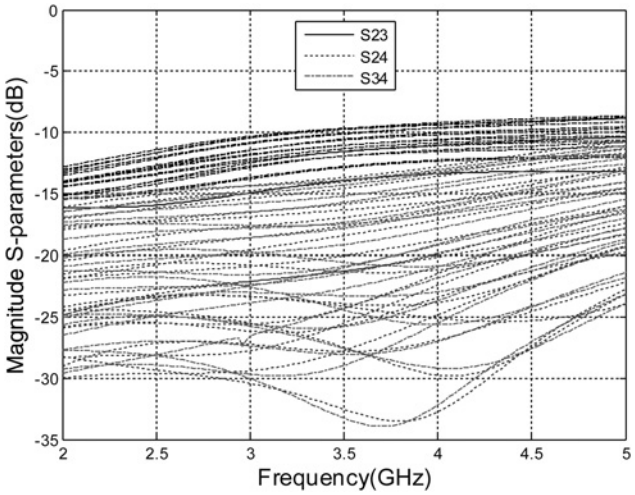

Fig. 9 *Simulated isolation between the output ports for different values of the varactors' capacitors*

The measured performance of the developed device is shown in Figs. 10–12 for biasing voltages of the two utilised diodes that change from 2.5 to 15 V. The results of Fig. 10 concerning the ratio of the signals at the three output ports, which are shown for small number of biasing voltages steps for clarity of the figure, agree well with the simulated results (Fig. 7). The selected biasing voltages shown in Fig. 10 are chosen based on the technical data of the diodes so that their capacitors are roughly equal to those used to obtain the simulated results of Fig. 7 to enable a comparison between them. The obtained results indicate the possibility of controlling the signal ratio at the three output

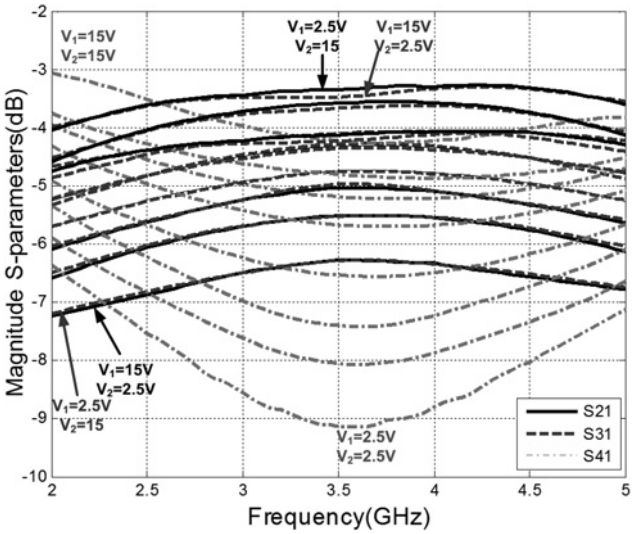

Fig. 10 *Measured signal level at the three output ports for different values of the varactors' biasing voltages*

doi: 10.1049/iet-map.2012.0124

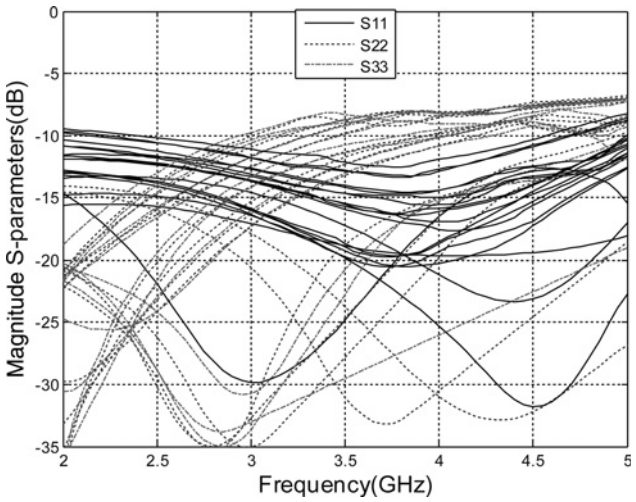

Fig. 11 *Measured reflection coefficient at the input and output ports for different values of the varactors' biasing voltages*

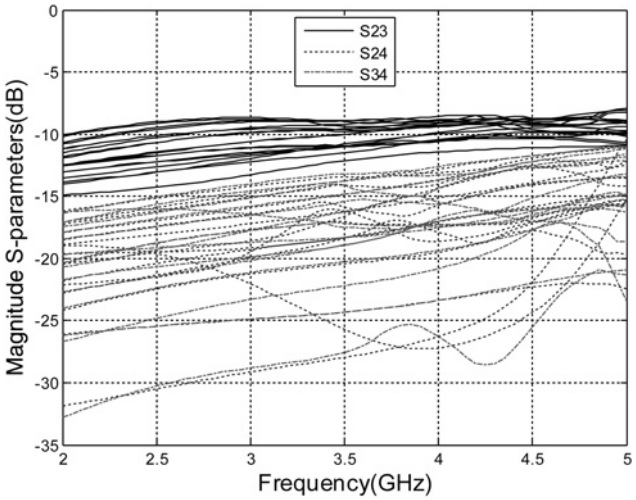

Fig. 12 *Measured isolation between the output ports for different values of the varactors' biasing voltages*

ports by a factor of around 2.8, which is close to the value 3 used in the design procedure. The deviation in the output signal values is around ± 1 dB from the median value of each ratio across the band from 2 to 5 GHz.

The measured reflection coefficient at the input port (port 1) of the device is below -10 dB as shown in Fig. 11. For the other two output ports, the reflection coefficient is less than -8 dB. For the configuration of transmitting array depicted in Fig. 1*b*, the reflection coefficient of the input port is the most important parameter among the reflection coefficients of the four ports as it quantifies the level of signal reflected back from the three-way signal divider to the amplifier. To avoid any disturbance to the operation of the amplifier, that signal should be as low as possible, which occurs when the input reflection coefficient is very low. For the output ports (2, 3 and 4), there is no signal entering the output ports when the device is used with transmitting antenna array depicted in Fig. 1*b*. Thus, the reflection coefficients at those ports are not critical parameter in the design compared with the input reflection coefficient.

As indicated in Fig. 12, there is also a good isolation of more than 12 dB between the output ports 2 and 4 or ports 3 and 4 in all the investigated cases. The isolation between the output ports 2 and 3 is more than 10 dB in most of the cases. As in the simulations, the only case that causes the isolation to be around 9 dB is when the biasing voltages at the varactor diodes are close to zero causing the varactor's capacitors to be at their maximum values. In this case, the coupling factor between the two side lines, which is assumed to be zero in the design, has a certain non-zero value that causes a slight degradation in the isolation between the two-side lines.

Comparing the simulated results in Figs. 7–9 with the measured results in Figs. 10–12 reveals a good agreement between them. The slight differences are thought to be owing to the parasitic elements of the utilised varactor diodes and the imperfect isolation between the biasing circuit and the coupled structure.

The other important factor to evaluate the proposed device is the phase performance. For the application intended in the work, that is, the amplitude–weight pattern optimisation of a transmitting array, the difference in the phase between the three output ports of the signal divider should have a certain fixed value across the band of interest so that no additional variable phase compensation techniques are needed. Concerning the designed device, the differential phase of the ports 2 and 3 with respect to port 4 are calculated using the simulation tool and measured. Snapshots of the results are shown in Fig. 13 for three cases that represent the two ends of the operating conditions of the device and the central design working condition. It is clear from the results that the ports 2 and 3 have an average 90° in the simulations and 92° in the measurements fixed phase difference with respect to port 4. The deviation in that phase difference is around $\pm 6^\circ$ in the simulations and $\pm 8^\circ$ in the measured results across the investigated band. This result can be explained by the fact the coupled structures between the two output ports (2 and 3) and the input port (1) are in the form of a quadrature coupler, whereas the output port 4 is directly connected with the input port. Thus, the two ports (2 and 3) are in phase, whereas a fixed 90° phase shift is expected between them and the other output port (4).

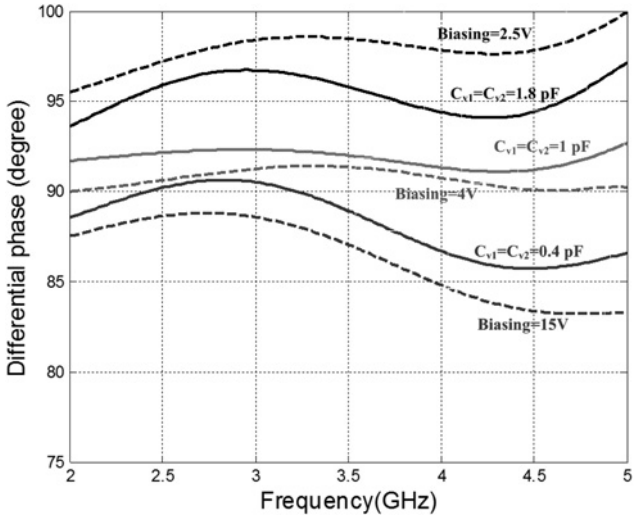

Fig. 13 *Simulated and measured differential phase of port 2 (or similarly port 3) with respect to port 4 at the two ands and central point of the operating conditions as indicated*

Solid lines, simulations; dash lines, measurements

5 Conclusion

A wideband three-way signal divider with tunable amplitude ratio has been presented. The proposed device utilises a planar parallel-coupled configuration and two varactor diodes. Through changing the biasing voltage of the varactor diodes, the coupling factor is changed and thus the signal level at the three output ports is varied. The signal flow of multiport devices is used to explain the performance of the device, whereas the conformal mapping is used to find its dimensions. The simulated and measured results have shown the possibility of achieving wide range of signal levels at the three output ports across more than 85% fractional bandwidth. The proposed device is a good candidate for pattern optimisation of low-power transmitting antenna arrays.

6 References

1 Mailloux, R.: 'Phased array antenna handbook' (Artech House, 2005, 2nd edn.)
2 Haupt, R.: 'Antenna arrays: a computational approach' (Wiley-IEEE Press, 2010)
3 Kohno, R.: 'Spatial and temporal communication theory using adaptive antenna array', *IEEE Pers. Commun.*, 1998, **5**, (1), pp. 28–35
4 Li, Y., Jandhyala, V.: 'Design of retrodirective antenna arrays for short-range wireless power transmission', *IEEE Trans. Antennas Propag.*, 2012, **60**, (1), pp. 206–211
5 Vaillancourt, R.: 'Analysis of the variable-ratio microwave power divider', *IRE Trans. Microw. Theory Tech.*, 1958, **6**, (2), pp. 238–239
6 Chao, G.: 'A wide-band variable microwave coupler', *IEEE Trans. Microw. Theory Tech.*, 1970, **18**, (9), pp. 576–583
7 Ferrero, F., Luxey, C., Staraj, R., Jacquemod, G., Yedlin, M., Fusco, V.: 'Theory and design of a tunable quasi-lumped quadrature coupler', *Microw. Opt. Technol. Lett.*, 2009, **51**, (9), pp. 2219–2222
8 Yeung, L.: 'A compact directional coupler with tunable coupling ratio using coupled-line sections'. Asia-Pacific Microwave Conf., Melbourne, 2011, pp. 1730–1733
9 Abbosh, A.: 'Ultra-wideband three-way power divider using broadside-coupled microstrip-coplanar waveguide', *Microw. Opt. Technol. Lett.*, 2012, **54**, (1), pp. 196–199
10 Oraizi, H., Ayati, S.-A.: 'Optimum design of broadband n-way rectangular power dividers with arbitrary power division and impedance matching', *IET Microw. Antennas Propag.*, 2011, **5**, (12), pp. 1447–1454
11 Abbosh, A.: 'Multilayer inphase power divider for UWB applications', *Microw. Opt. Technol. Lett.*, 2008, **50**, (5), pp. 1402–1405
12 Abbosh, A.: 'Ultra wideband inphase power divider for multilayer technology', *IET Microw. Antennas Propag.*, 2009, **3**, (1), pp. 148–153
13 Wong, S., Zhu, L.: 'Ultra-wideband power dividers with good isolation and improved sharp roll-off skirt', *IET Microw. Antennas Propag.*, 2009, **3**, (8), pp. 1157–1163
14 Song, K., Xue, Q.: 'Ultra-wideband 12-way coaxial waveguide power divider with rotated electric field mode', *IET Microw. Antennas Propag.*, 2011, **5**, (5), pp. 512–518
15 Abbosh, A.: 'Three-way parallel-coupled microstrip power divider with ultrawideband performance and equal-power outputs', *IEEE Microw. Wirel. Compon. Lett.*, 2011, **21**, (12), pp. 649–651
16 Abbosh, A.: 'Design of ultra-wideband three-way arbitrary power dividers', *IEEE Trans. Microw. Theory Tech.*, 2008, **56**, (1), pp. 194–201
17 Kishihara, M., Ohta, I., Yamane, K.: 'Multi-stage, multi-way microstrip power dividers with broadband properties', *IEICE Trans. Electron.*, 2006, **E89-C**, pp. 622–629
18 Tahara, Y., Oh-hashi, H., Miyazaki, M., Makinoet, S.: 'A broadband three-way tapered-line power divider with several strip resistors'. Proc. 35th Europe Microwave Conf., 2005, vol. 1, pp. 49–52
19 Abbosh, A.: 'Closed-form design method for tight parallel-coupled microstrip coupler with ultra-wideband performance and practical dimension', *Electron. Lett.*, 2011, **47**, (9), pp. 547–549
20 Abbosh, A.: 'Design method for ultra-wideband bandpass filter with wide stopband using parallel-coupled microstrip lines', *IEEE Trans. Microw. Theory Tech.*, 2012, **60**, (1), pp. 31–38
21 Abbosh, A.: 'Analytical closed-form solution for different configurations of parallel-coupled microstrip lines', *IET Microw. Antennas Propag.*, 2009, **3**, (1), pp. 137–147
22 Collin, R.: 'Foundations for microwave engineering' (Wiley-IEEE Press, 2001, 2nd edn.)

doi: 10.1049/iet-map.2012.0124